

**$\beta$  decay and mass of the new neutron-rich isotope  $^{53}\text{Ti}^\dagger$** L. A. Parks,\* C. N. Davids,<sup>†</sup> and R. C. Pardo<sup>§</sup>*Physics Division, Argonne National Laboratory, Argonne, Illinois 60439*

(Received 8 October 1976)

The new isotope  $^{53}\text{Ti}$  has been produced with the  $^{48}\text{Ca}(^7\text{Li},pn)^{53}\text{Ti}$  reaction at  $E_{^7\text{Li}} = 14\text{--}20$  MeV. The  $\beta$ -decay scheme of  $^{53}\text{Ti}$  was determined from  $\gamma$ -ray singles and  $\gamma$ - $\gamma$  coincidence experiments using high-resolution Ge(Li) and intrinsic germanium detectors. The four strongest decay  $\gamma$  rays have energies of 100.8, 127.6, 228.4 (all  $\pm 0.1$ ), and 1675.5  $\pm 0.3$  keV, with relative intensities of  $50.9 \pm 2.7$ ,  $115.4 \pm 12.0$ , 100, and  $62.5 \pm 6.7$ , respectively. The  $^{53}\text{Ti}$  half-life was determined to be  $32.7 \pm 0.9$  sec. Three new levels with excitation energies of 1958, 2550, and 2931 keV were observed in the daughter  $^{53}\text{V}$ . The total  $^{53}\text{Ti}$  decay energy of  $5.02 \pm 0.10$  MeV was measured by performing a  $\beta$ - $\gamma$  coincidence experiment using a plastic scintillation detector for the  $\beta$  rays. This yields a  $^{53}\text{Ti}$  mass excess of  $-46.84 \pm 0.10$  MeV. The decay scheme provides  $J^\pi$  restrictions for the observed states of  $^{53}\text{V}$ , and these are compared with previous measurements and shell model calculations. The measured mass of  $^{53}\text{Ti}$  is compared with various predictions.

RADIOACTIVITY  $^{53}\text{Ti}$  [from  $^{48}\text{Ca}(^7\text{Li},pn)$ ]; measured  $T_{1/2}$ ,  $E_\gamma$ ,  $I_\gamma$ ,  $E_\beta$ ,  $\gamma$ - $\gamma$  coin,  $\beta$ - $\gamma$  coin; deduced decay scheme,  $\log ft$ , mass excess.  $^{53}\text{V}$  deduced levels,  $J^\pi$  restrictions,  $\pi$ . Enriched targets, multiple rabbit facility; Ge(Li), intrinsic Ge, and plastic detectors.

## I. INTRODUCTION

A program of investigating the decay properties of nuclei far from the valley of  $\beta$  stability has been initiated at the Argonne National Laboratory (ANL) FN tandem Van de Graaff accelerator facility. One group of new isotopes which is presently being investigated is the  $T_z = -\frac{3}{2}$  species which can be made by heavy-ion induced reactions on  $^{48}\text{Ca}$ . The measurements of the masses of these nuclei will present a good test for the predictions of the various mass formulas in the  $f$ - $p$  shell. The study of the previously observed decay of  $^{51}\text{Sc}$  has recently been completed.<sup>1</sup> The present study focuses on the  $\beta$  decay of the isotope  $^{53}\text{Ti}$ .

Neutron-rich nuclei in the  $50 < A < 70$  mass region are of importance in several astrophysical aspects. The nucleosynthesis of the rare, stable, neutron-rich isotopes in this region is thought to occur during explosive carbon burning in a supernova explosion.<sup>2</sup> Calculations of such events require the neutron separation energies for the stable, as well as the unstable nuclides in this mass region.

It is thought that a neutron star is formed from a supernova remnant by the neutronization of the dense hot core of an exploding massive star.<sup>3</sup> Neutron-rich nuclei may exist on the surface of the remnant due to direct captures of degenerate electrons on abundant iron peak nuclei. Not only are nuclear masses important for neutron star crust calculations, but information concerning the structures of the nuclear states, as well as

the  $\log ft$  values of the  $\beta$  decays, is also needed.

Hinds, Marchant, and Middleton<sup>4</sup> first studied the excited states of  $^{53}\text{V}$ , the daughter of  $^{53}\text{Ti}$ , via the  $^{51}\text{V}(t,p)^{53}\text{V}$  reaction at 12.09 MeV. The angular distributions of the protons yielded  $l$ -value transfers to excited states of  $^{53}\text{V}$ . Pronko, Bardin, and Becker<sup>5</sup> studied low-lying levels in  $^{53}\text{V}$  via the reaction  $^{51}\text{V}(t,p\gamma)^{53}\text{V}$  at a bombarding energy of 2.9 MeV.  $\gamma$ -ray decay modes were studied, and lifetimes of many of the states were measured using both the Doppler-shift attenuation method and direct timing. Proton- $\gamma$ -ray coincidence experiments were also performed. These measurements aided in specifying the possible  $J^\pi$  assignments to the states observed in  $^{53}\text{V}$ .

Shell-model calculations of the  $Z = 20\text{--}28$  and  $N = 30$  isotones using effective nucleon-nucleon interactions have been previously performed by Vervier,<sup>6,7</sup> McGrory,<sup>8</sup> and Horie and Ogawa.<sup>9</sup> Horie and Ogawa<sup>9</sup> predicted the energies and  $J^\pi$  values of low-lying states in  $^{53}\text{V}$  by assuming that  $^{53}\text{V}$  is composed of an inert  $^{48}\text{Ca}$  core with the three valence protons allowed to occupy the  $1f_{7/2}$  shell. The two valence neutrons were allowed to occupy the  $2p_{3/2}$ ,  $1f_{5/2}$ , and  $2p_{1/2}$  shells.  $^{48}\text{Ca}$  core excitations were not included in their calculations. The single-particle energies and effective nucleon-nucleon interaction matrix elements were obtained from experimental data.

The single-particle shell model predicts the ground state  $J^\pi$  of  $^{53}\text{Ti}_{31}$  to be  $\frac{3}{2}^-$  due to the  $\pi(f_{7/2})^2\nu(p_{3/2})^{-1}$  configuration. The following discussions of the decay of  $^{53}\text{Ti}$  assume a ground-state spin and parity of  $\frac{3}{2}^-$ .

## II. APPARATUS

The decay properties of  $^{53}\text{Ti}$  were studied by observing its  $\beta$  rays and  $\beta$ -delayed  $\gamma$  rays.  $\beta$  rays were observed with a plastic scintillation detector, and high-resolution Ge(Li) and intrinsic germanium detectors were used to observe the  $\gamma$  rays.

All of the spectroscopy was performed in a well-shielded area. The activated target was transferred to and from this area with a pneumatic target-transfer system ("rabbit").<sup>10</sup> By doing so, the background from the contaminated beam line was eliminated, and the Ge(Li) detectors were shielded from possible damage by the neutron flux present during the bombardment of the target.

One of the major disadvantages of investigating short-lived  $\beta$ -unstable nuclei produced by heavy-ion induced reactions using such a rabbit system is that many other longer-lived species are usually produced. Since the bombard-count cycle is repeated many times during an experiment, the long-lived activities tend to build up in the target. This creates a background problem for the detection of the  $\gamma$  and  $\beta$  rays from the shorter-lived nuclei. With this problem in mind, a multiple-rabbit transfer system<sup>10</sup> was constructed for the study of short-lived isotopes. Its basic function is to automatically remove the previously bombarded target from the experiment after the counting and replace it with a relatively fresh target.

The multiple- and single-rabbit systems transfer the target in an identical fashion. The only difference between the two systems is at the beam end of the system. In the multiple system, up to eight targets are placed in holders of the same dimensions as that of the rabbit tube. The holders are mounted on a carousel disk arrangement which rotates a fresh target into position just prior to bombardment. This allows the target activity to decay for seven cycles. Further details may be found in Ref. 10.

The reaction  $^{48}\text{Ca}(^7\text{Li},pn)^{53}\text{Ti}$  was used to form  $^{53}\text{Ti}$ . Data were taken at lab bombarding energies of 14, 16, 18, and 20 MeV, with target currents typically from 50 to 100 nA (electrical) using the 3+ charge state of the  $^7\text{Li}$ .

Early runs were done using the single rabbit and the later data were taken using the multiple rabbit. The  $^{48}\text{Ca}$  targets used in the initial single-rabbit experiments were made by evaporating approximately 200  $\mu\text{g}/\text{cm}^2$  of Ca enriched to 96.78% in  $^{48}\text{Ca}$  onto a 0.013-mm-thick Au backing mounted on a delrin target holder. Approximately 100  $\mu\text{g}/\text{cm}^2$  of Au was then evaporated onto the  $^{48}\text{Ca}$  so that the target could be easily handled and be protected from oxidation. For the multiple-rabbit experiments the targets were similar, except that the

$^{48}\text{Ca}$  was in the form of 1.17  $\text{mg}/\text{cm}^2$ -thick rolled foils.

Ge(Li) detectors having crystal volumes of 66.4 and 82  $\text{cm}^3$  were used for the detection of the  $\gamma$  rays. Their energy resolutions during the experiments were measured to be 2.2 to 2.3 keV full width at half maximum (FWHM) for the 1.333-MeV  $^{60}\text{Co}$   $\gamma$  ray. A 2.5-cm-thick polyethylene absorber was placed between the Ge(Li) detector and the rabbit tube counting window. The absorber served to stop  $\beta$  rays with energies up to 6 MeV which would otherwise be free to interact with the detector crystal and contribute to the background.

A 100-mm<sup>2</sup>  $\times$  10-mm-deep intrinsic germanium detector was used to observe low-energy  $\gamma$  rays and x rays. Its energy resolution was measured to be 600 eV FWHM for the 122-keV  $^{57}\text{Co}$   $\gamma$  ray. Absorbers were not used with this detector.

For the detection of the  $\beta$  rays, a 7.0-cm-diam by 4.4-cm-deep NE102 plastic scintillator tapered at the bottom was coupled to an RCA 8575 photomultiplier tube. The areal density of the material between the activated target and the scintillator plastic was 47  $\text{mg}/\text{cm}^2$  and created a calculated minimum energy loss of 80 keV for a 3-MeV electron.

## III. EXPERIMENTAL PROCEDURE

To determine the half-life of  $^{53}\text{Ti}$ , the decays of its strongest  $\beta$ -delayed  $\gamma$  rays were monitored. This was done by routing the  $\gamma$ -ray pulses from the Ge(Li) detector into six successive 4096-channel "time bins" of 20-s accumulation time. A constant-frequency pulser signal was injected into the Ge(Li) detector preamplifier in order to monitor the dead time in the analog-to-digital converter, computer, and associated electronics.

The 127-keV  $\gamma$  ray ascribed to the decay of  $^{53}\text{Ti}$  could not be resolved from the very intense 124-keV  $\gamma$  ray from the decay of  $^{52}\text{Ti}$ . The half-life of the 127-keV  $\gamma$  ray was measured by routing into the time bins all  $\gamma$  rays in coincidence with  $\beta$  rays with energies larger than approximately 1.4 MeV. By requiring such a  $\beta$ -ray threshold, the 124-keV  $\gamma$  ray was greatly attenuated since the state of  $^{52}\text{V}$  producing this  $\gamma$  ray corresponds to a  $^{52}\text{Ti}$  decay energy of 1.83 MeV.<sup>11</sup>

A  $\gamma$ - $\gamma$  coincidence experiment was performed using two Ge(Li) detectors placed opposite one another with the counting windows of the rabbit tube situated between them. A coincidence resolving time of 60 ns was used in order to enhance the low-energy coincident  $\gamma$ -ray detection efficiency.

A  $\beta$ - $\gamma$  coincidence experiment was performed

with the Ge(Li) and scintillation detectors placed in the same geometry as the detectors in the  $\gamma$ - $\gamma$  coincidence experiment. A pileup gate was used on the scintillator timing discriminator to eliminate pulse-pileup problems due to high count rates. Whenever a pileup occurred, analysis of the corresponding linear signals was inhibited. The coincidence timing window was set to a width of 30 ns. A delay-line amplifier was used to shape the linear signals from the scintillation detector to a width of 0.5  $\mu$ s. Singles count rates in the Ge(Li) and the scintillation detectors were 3000 to 4000 cps and 20 000 to 30 000 cps, respectively. The coincident count rate was between 600 to 1000 cps. No significant  $\beta$ -ray gain shifts were observed as a function of high, varying count rates in the scintilla-

tor. Data taken during both the  $\beta$ - $\gamma$  and  $\gamma$ - $\gamma$  coincidence experiments were stored event by event on magnetic tape for subsequent off-line analysis.

#### IV. RESULTS

##### A. Half-life and decay scheme

It was found that  $^{53}\text{Ti}$  had been produced by  $^7\text{Li}$  bombardment of  $^{48}\text{Ca}$  when the relatively strong  $\beta$ -delayed  $\gamma$  rays with energies of 101, 127, and 228 keV were observed. These energies agreed with observations from the  $^{51}\text{V}(t, p\gamma)^{53}\text{V}$  study done by Pronko *et al.*<sup>5</sup> In addition, it was found that these three  $\gamma$  rays all decayed with a half-life near 30 s.

The half-life of the decay of  $^{53}\text{Ti}$  was determined

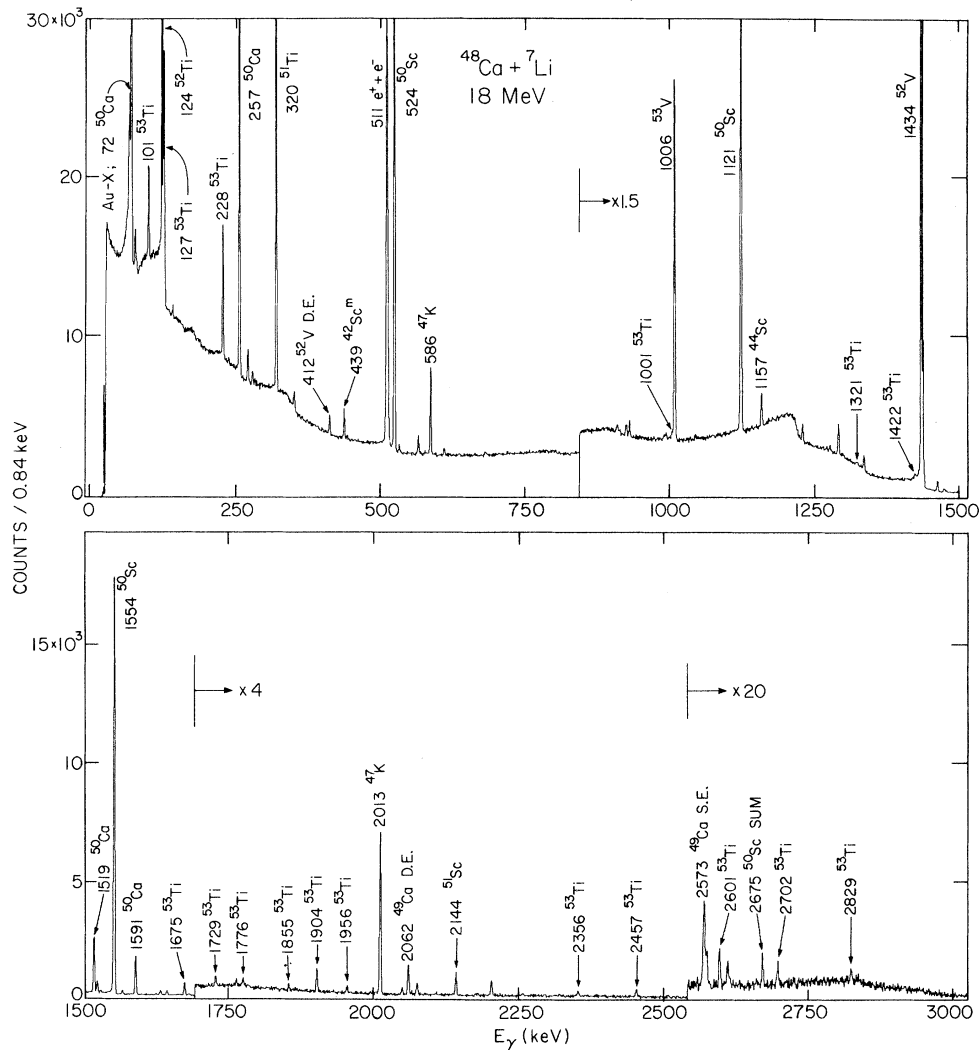


FIG. 1.  $\beta$ -delayed  $\gamma$ -ray singles spectrum taken at 18 MeV with the Ge(Li) detector. The  $^{53}\text{Ti}$  decay  $\gamma$  rays as well as prominent  $\gamma$  rays from the decays of contaminant isotopes are identified. Computer overflow is seen in some of the central channels for the most intense peaks.

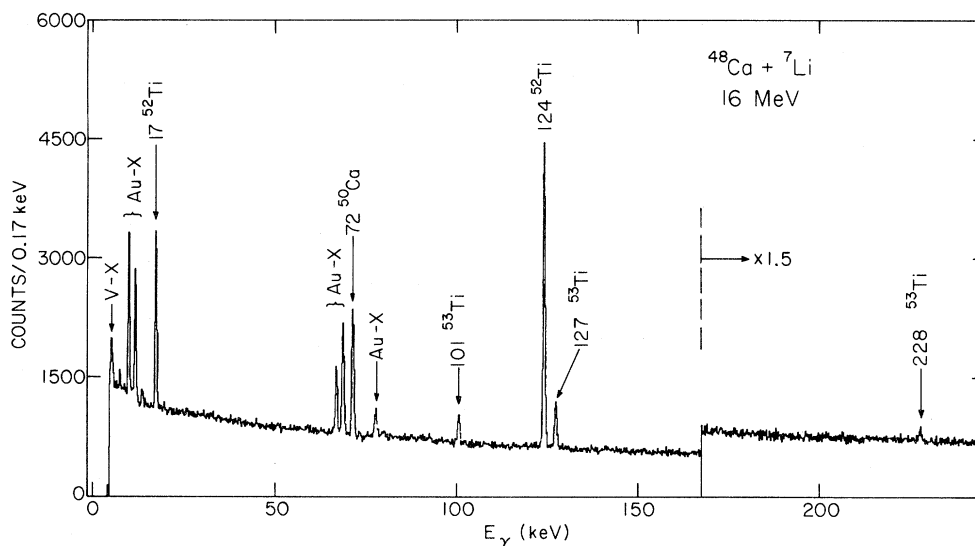


FIG. 2.  $\beta$ -delayed  $\gamma$ -ray singles spectrum taken at 16 MeV with the intrinsic germanium detector. The  $^{53}\text{Ti}$  decay  $\gamma$  rays as well as prominent  $\gamma$  rays from the decays of contaminant isotopes are identified. Observed x rays are also identified. The Au x rays are from the Au target backings.

by following the decays of the  $\beta$ -delayed 101-, 127-, and 228-keV  $\gamma$  rays. After correction for dead time, the composite decay curve for these three  $\gamma$  rays yielded a half-life of  $32.7 \pm 0.9$  s. It was assumed that  $^{53}\text{Sc}$  was not produced to any significant degree by the improbable  $^{48}\text{Ca}(^7\text{Li}, 2p)\text{-}^{53}\text{Sc}$  reaction. This assumption rules out the possible production of  $^{53}\text{Ti}$  by the  $\beta$  decay of  $^{53}\text{Sc}$ .

Figure 1 shows the  $\gamma$ -ray singles spectrum obtained with the Ge(Li) detector. The spectrum was obtained by bombarding the target for 5 s and then counting for 40 s, using the multiple rabbit. Figure 2 is the spectrum obtained with the intrinsic germanium detector. Table I summarizes the energies and relative intensities obtained for the  $\gamma$  rays associated with the decay of  $^{53}\text{Ti}$ . All  $\gamma$ -ray intensities were normalized directly to the intensity of the 228-keV  $\gamma$  ray and corrected for coincident summing. The relative intensities of the 1001-, 1321-, 1422-, and the two 2702-keV  $\gamma$  rays were obtained from the  $\gamma$ - $\gamma$  coincidence data since they could not be adequately resolved in the  $\gamma$ -ray singles data.

To determine which  $\gamma$  rays were in coincidence with the  $^{53}\text{Ti}$  decay  $\gamma$  rays, digital windows were set on the  $\gamma$ -ray peaks observed in the total coincident  $\gamma$ -ray spectrum of detector 1. Digital gates were also set on background areas on both sides of the peaks. Events in detector 2 were sorted according to these gates, and the appropriate background subtractions were made. Table II shows the resulting coincidence matrix involving the decay  $\gamma$  rays of  $^{53}\text{Ti}$ .

The decay scheme of  $^{53}\text{Ti}$  was determined from

the  $\gamma$ - $\gamma$  coincidence data, the relative intensities and energies of the decay  $\gamma$  rays, and the previous  $^{51}\text{V}(t, p)^{53}\text{V}$  studies.<sup>4,5</sup> Figure 3 is the  $^{53}\text{Ti}$  decay scheme obtained from this study. All excitation energies have been corrected for nuclear recoil.

Assuming that the decay of  $^{53}\text{Ti}$  proceeds by allowed  $\beta$  transitions, the states directly populated in  $^{53}\text{V}$  should have  $J^\pi$  values of only  $\frac{1}{2}^-$ ,  $\frac{3}{2}^-$ , or  $\frac{5}{2}^-$ . The ground state  $J^\pi$  of  $^{53}\text{V}$  has been observed to

TABLE I.  $\gamma$  rays observed in the decay of  $^{53}\text{Ti}$ .

$E_\gamma$ (keV)	$I_\gamma$ (rel.)
$100.8 \pm 0.1$	$50.9 \pm 2.7$
$127.6 \pm 0.1$	$115.4 \pm 12.0$
$228.4 \pm 0.1$	100
$679.6 \pm 1.3$	$10.1 \pm 2.0$
$1001.0 \pm 1.1$	$11.3 \pm 3.2$
$1033.1 \pm 1.8$	$6.4 \pm 2.3$
$1321.1 \pm 1.5$	$15.1 \pm 2.6$
$1421.7 \pm 0.9$	$26.5 \pm 3.4$
$1675.5 \pm 0.3$	$62.5 \pm 6.7$
$1729.2 \pm 0.6$	$12.1 \pm 1.8$
$1776.5 \pm 0.7$	$10.2 \pm 1.4$
$1855.5 \pm 0.7$	$8.1 \pm 1.3$
$1904.0 \pm 0.3$	$31.0 \pm 2.1$
$1956.4 \pm 0.5$	$8.7 \pm 1.1$
$2355.5 \pm 0.6$	$7.7 \pm 1.3$
$2456.6 \pm 0.5$	$13.4 \pm 1.3$
$2601.0 \pm 0.4$	$15.5 \pm 2.0$
$2702 \pm 2$	$7.2 \pm 1.4$
$2702 \pm 2$	$2.4 \pm 0.7$
$2829.1 \pm 2.2$	$5.1 \pm 1.1$

TABLE II. Gated versus coincident  $^{53}\text{Ti}$  decay  $\gamma$  rays. A denotes not observed due to poor statistics. B denotes not observed due to competition from backscatter peak. C denotes possible observation. X denotes definite coincidence.

Gated $\gamma$ rays (keV)	Coincident $\gamma$ rays (keV)																	
	101	127	228	679	1001	1033	1321	1422	1675	1729	1776	1855	1904	1956	2356	2457	2601	2702
101		X		X	A	A	C		X	X		X			X		X	A
127	X			X	X	X	X	X	X	X	X			X	X	X	X	X
228				X	X	A	B		X	X		X			X		X	X
679	A	X	A						X		A		X					
1001	X	X	X				C	X										
1033	A	X	A				X	X										
1321	C	X	B		C	A												
1422		X			X	X												
1675	X	X	X	X														
1729	X	X	X															
1776		X		A														
1855	X	X	X															
1904				X														
1956		X																
2356	X	X	X															
2457		X																
2601	X	X	X															
2702	X	X	X															

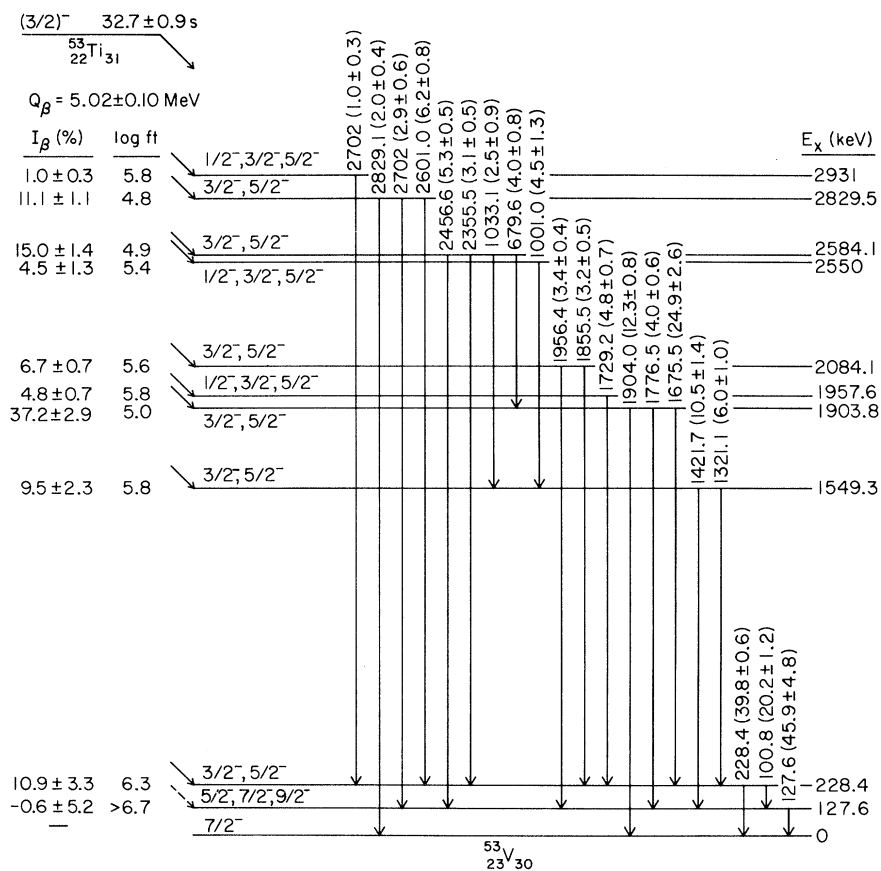


FIG. 3. Decay scheme of  $^{53}\text{Ti}$ . The  $J^\pi$  assignments of states in  $^{53}\text{V}$  are based upon the assumption that the ground state  $J^\pi$  of  $^{53}\text{Ti}$  is  $3/2^-$  and on  $l$ -transfer values observed in the  $^{51}\text{V}(t, p)^{53}\text{V}$  study by Ref. 4. Internal conversion is assumed to be negligible. The  $\gamma$ -ray intensities are the numbers observed per 100 disintegrations.

be  $\frac{7}{2}^-$ .<sup>4</sup>

The  $J^\pi$  assignment of  $\frac{1}{2}^-$  to any state which decays by  $\gamma$ -ray emission directly to the ground state is very unlikely since this would require an  $M3$   $\gamma$ -ray transition. Such a transition is not expected to be competitive if an  $E2$  or  $M1$  transition can occur through an intermediate state. Also, every state except the 1957-, 2250-, and 2931-keV states was observed in the  $^{51}\text{V}(t, p)^{53}\text{V}$  study by Hinds *et al.*<sup>4</sup> The largest  $l$  transfer they observed to these states was  $\Delta l = 2$ , thus setting a  $J^\pi$  lower limit of  $\frac{3}{2}^-$  to these states. An  $l$ -transfer value was not determined for the 2829-keV state.

On the basis of the  $l = 2$  transfer observed for the first excited state in the  $^{51}\text{V}(t, p)^{53}\text{V}$  study,<sup>4</sup> this state is given possible  $J^\pi$  values of  $\frac{3}{2}^-$  to  $\frac{11}{2}^-$ , inclusive. The  $\beta$ -decay study cannot provide further restrictions since the state is apparently not fed by  $\beta$  decay. Pronko *et al.*<sup>5</sup> measured the lifetime of the state to be  $\leq 1$  ns. This would require a very large  $E2$  transition strength of 2000 single-particle units for the ground-state transition. Because of this unreasonably large enhancement, the possible  $J^\pi$  assignments of  $\frac{3}{2}^-$  and  $\frac{11}{2}^-$  for the 127-keV state are eliminated.

The  $\beta$  branches to states in  $^{53}\text{V}$  were obtained from the  $\gamma$ -ray intensity balance for each state. Branching to the ground state is assumed to be negligible since such a feeding would come from a forbidden  $\beta$  decay. Internal conversion affecting the inferred  $\beta$  branches was neglected due to the low atomic number of  $^{53}\text{V}$  and the relatively high energies of the decay  $\gamma$  rays. It is assumed that the 101- and 127-keV transitions are  $M1$ . However, there will be a significant effect if these are  $E2$  transitions. This effect will be discussed more fully below.

$\text{Log}ft$  values were calculated using the  $\beta$  branches, the  $^{53}\text{Ti}$  decay half-life of 32.7 s, and a total decay energy of 5.02 MeV (see below).  $\text{Log}f$  values were obtained from the tables by Gove and Martin.<sup>12</sup>

#### B. Mass excess of $^{53}\text{Ti}$

The  $\beta$ - $\gamma$  coincidence experiment was performed in order to measure the total decay energy of  $^{53}\text{Ti}$ . This was done by determining the end-point energies of  $\beta$  spectra in coincidence with several of the  $^{53}\text{Ti}$  decay  $\gamma$  rays after having determined the decay scheme.

To obtain the coincident  $\beta$  spectra, digital gates were set on several  $\beta$ -coincident  $\gamma$ -ray peaks and background corrections were made to the resultant spectra.

To obtain internal end-point calibrators,  $\beta$  spectra from the decays of known isotopes observed in

the same experiment were obtained. Appropriate  $\gamma$  rays were gated so that the  $\beta$  spectra thus obtained were relatively pure. That is, there was little or no unwanted  $\beta$  contributions due to feedings of higher states in subsequent coincidence with the gated  $\gamma$  rays. Coincident  $\gamma$  rays contributed negligible amounts to the spectra and were usually neglected. The  $\beta$  spectra thus obtained are all attributed to allowed transitions with the daughters' atomic numbers ranging from 19 to 23.

The  $\beta$  spectrum coincident with the 1434-keV  $\gamma$  ray from the decay of strongly produced  $^{52}\text{V}$  was obtained. The spectrum is very pure since 99% of the decay of  $^{52}\text{V}$  feeds the 1434-keV first-excited state of  $^{52}\text{Cr}$ .<sup>13</sup> A hand-drawn curve, termed the "standard shape," was drawn through the points in the spectrum producing an empirical description of the spectral shape. Figure 4 shows the experimentally obtained  $^{52}\text{V}$   $\beta$  spectrum and the standard shape.

To test the validity of the standard shape in describing the experimentally obtained spectrum, a least-squares program was used to fit the standard shape to the spectrum. Points from the standard shape were used in place of an analytical function. To fit the standard shape to the spectrum, two free parameters which altered the height and either stretched or compressed the curve along the abscissa were varied by the program until the  $\chi^2$  minimum was reached.

After determining that the standard shape quite adequately represented the  $^{52}\text{V}$  spectrum, the same procedure was used to fit the standard shape

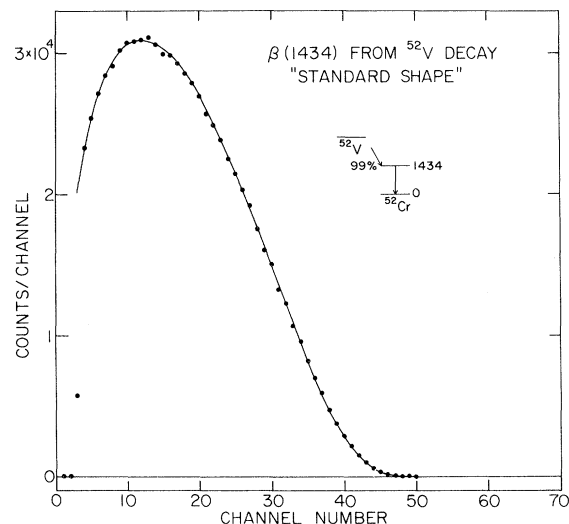


FIG. 4. Background-corrected  $\beta$  spectrum from the decay of  $^{52}\text{V}$  to the 1434-keV first excited state in  $^{52}\text{Cr}$ . The "standard shape" is a hand-drawn curve chosen to describe the spectrum.

TABLE III. Information concerning the  $\beta$  spectra used for the stretch fitting technique calibration.

Isotope	$E_\gamma$ (keV)	$E_{\max}^\beta$ (keV)	Ref.	Stretch factor	Fitting region (Channel Nos.)	$\chi_p^2$
$^{52}\text{V}$	1433.9	$2544.8 \pm 2.9$	a, b	$1.000 \pm 0.001$	4–44	1.07
$^{53}\text{V}$	1006.0	$2417.3 \pm 25.1$	b, c	$0.946 \pm 0.002$	4–38	0.91
$^{51}\text{Ti}$	$319.9^d$	$2145.4 \pm 3.4$	b	$0.831 \pm 0.002$	4–34	1.01
	$928.2^d$	$1537.0 \pm 3.5$	b	$0.544 \pm 0.084$	4–17	1.52
$^{50}\text{Ca}$	1591.0	$3120.1 \pm 17.9$	b, e	$1.252 \pm 0.009$	4–50	0.91
	1519.4	$3120.1 \pm 17.9$	b, e	$1.252 \pm 0.010$	5–50	0.98
$^{49}\text{Ca}$	3084.4	$2183.5 \pm 6.4$	b, f	$0.835 \pm 0.009$	5–29	1.01
$^{47}\text{K}$	585.8	$4045.1 \pm 8.8$	b, e	$1.636 \pm 0.007$	5–65	1.43

<sup>a</sup>Reference 13.

<sup>b</sup>A. H. Wapstra, K. Bos, and N. B. Gove, 1974 Supplement to the 1971 Atomic Mass Adjustment (private communication, F. J. D. Serduke).

<sup>c</sup>L. Donikens-Vanpraet, M. Dorikens, and J. Demnynck, *Z. Phys.* **241**, 459 (1971).

<sup>d</sup> $E_\gamma$  obtained from present work.

<sup>e</sup>E. K. Warburton, D. E. Alburger, and G. A. P. Engelbertink, *Phys. Rev. C* **2**, 1427 (1970).

<sup>f</sup>E. Eichler and S. Raman, *Phys. Rev. C* **3**, 2268 (1971).

to the pure  $\beta$  spectra obtained for some of the other strongly produced isotopes. Table III lists the isotopes whose  $\beta$  spectra were fitted using this technique, the coincident decay  $\gamma$  rays, the known  $\beta$  end-point energies, and the abscissa stretch factors obtained. The fitting regions and the reduced  $\chi^2$  of the fits are also listed. A linear least-squares fit was made to the resulting plot of stretch factor vs known endpoint energy, shown in Fig. 5. It is obvious from this figure that the stretch fitting procedure was quite acceptable in determining end-point energies for stretch factors between 0.6 and 1.6. The lower portion of the fit is dotted since it is not certain that this accurately describes the true state of affairs for such low stretch factors. The linear fit was used as an energy calibration for specified stretch factors.

Background-corrected  $\beta$  spectra in coincidence with the 1675-, 1904-, 2356-, 2457-, and 2601-keV  $^{53}\text{Ti}$  decay  $\gamma$  rays were obtained. The spectra coincident with the 1675- and 1904-keV  $\gamma$  rays were added, as were those from the 2356- and 2457-keV  $\gamma$ -ray gates. The small  $\beta$  contribution from the feeding of the 2584-keV state in coincidence with the 1675- and 1904-keV  $\gamma$  rays, fed via the 679-keV  $\gamma$  ray, was subtracted from the summed  $\beta$  spectrum in coincidence with the 1675- and 1904-keV  $\gamma$  rays. Three relatively pure  $\beta$  spectra corresponding to the feedings of the 1904-, 2584-, and 2829-keV states in  $^{53}\text{V}$  were consequently obtained. The standard shape was fitted to the three spectra, and the stretch factors and end-point energies obtained are listed in Table IV. Also listed are the fitting regions used, the reduced  $\chi^2$  of the fits, and the  $^{53}\text{Ti}$  total decay energies subsequently obtained from the end-point energies of the feed-

ings to the three states. Figure 6 shows the fits to the spectra feeding the three states.

The resulting total decay energy of  $^{53}\text{Ti}$  is  $5.02 \pm 0.10$  MeV, corresponding to a  $^{53}\text{Ti}$  mass excess of  $-46.84 \pm 0.10$  MeV. The uncertainty includes a systematic uncertainty for the stretch procedure.

The major reason for using the stretch fitting technique is that most of the data points in the spectrum may be used in the fit procedure, as is obvious from the fitting regions specified in Tables III and IV. Historically,  $\beta$  end-point energies are usually extracted from Fermi-Kurie plots of the spectra. This technique has many drawbacks when a scintillation detector is used to collect the spec-

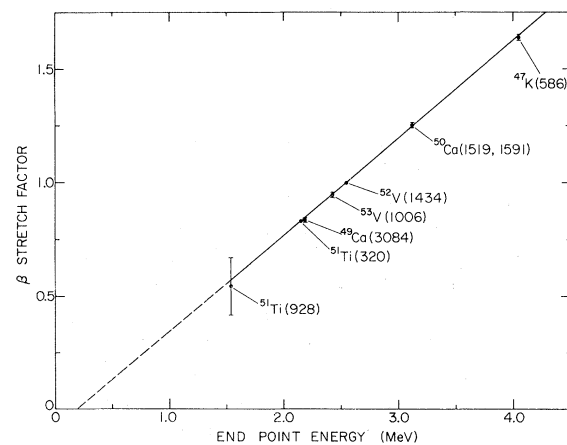


FIG. 5.  $\beta$  end-point energy calibration for the known, contaminant isotopes as a function of their stretch factors. The  $\gamma$  rays gated in order to obtain the coincident  $\beta$  spectra for the various isotopes are given. Information concerning the data points are summarized in Table III.

TABLE IV.  $\beta$  end-point energies to states in  $^{53}\text{V}$  and the corresponding  $^{53}\text{Ti}$  decay energies obtained using the stretch fitting technique.

$E_\gamma$ (keV)	$E_x$ (keV)	Stretch factor	$\chi_p^2$	Fitting region (Channel Nos.)	$E_{\max}^\beta$ (keV)	$Q_\beta$ (keV)
(1675 + 1904)						
- $f(679)$	1903.8	$1.247 \pm 0.030$	0.88	25–50 <sup>a</sup>	$3127 \pm 71$	$5031 \pm 71$
2356 + 2457	2584.1	$0.948 \pm 0.028$	1.00	4–38	$2423 \pm 65$	$5007 \pm 65$
2601	2829.5	$0.860 \pm 0.042$	0.72	4–35	$2217 \pm 99$	$5046 \pm 99$

<sup>a</sup>This smaller fitting region was used to limit the effect of possible systematic errors from the subtraction of the  $\beta$ -ray contributions via the 679-keV  $\gamma$  ray.

tra. The Fermi-Kurie plot deviates from linearity at the high-energy end of the plot due to the poor resolution qualities of the detector. Secondly, the low-energy end of the plot is highly distorted due to low-energy electron scattering. In the particular case of this study, greater deviations occur since the electrons must traverse the material between the activated target and the scintillator plastic. This creates relatively large energy losses and even poorer detector resolution. Due to these many limitations, a restricted number of data points must be used in the end-point energy determination. This means that the yields in the fitting regions usually have poor statistics and systematic errors may be introduced when choosing the linear fitting region.

Despite these objections, it was decided that Fermi-Kurie plots should be attempted for the internal calibrators and for the  $^{53}\text{Ti}$  spectra, and compared with the results obtained with the stretch fitting technique. The  $^{53}\text{Ti}$  total decay energy extracted using this technique was  $4.97 \pm 0.16$  MeV, in excellent agreement with the value obtained using the stretch technique. This value was not used in obtaining the  $^{53}\text{Ti}$  mass excess.

## V. DISCUSSION

Figure 7 summarizes the results of the decay study, the  $^{51}\text{V}(t, p)^{53}\text{V}$  study by Hinds *et al.*,<sup>4</sup> and the  $^{51}\text{V}(t, p\gamma)^{53}\text{V}$  study by Pronko *et al.*<sup>5</sup> Comparison is made with the shell-model calculation describing eigenstates in  $^{53}\text{V}$  done by Horie and Ogawa.<sup>9</sup> The dashed lines between the experimentally measured states and the calculated states are likely correlations. Higher states cannot be confidently correlated due to insufficient experimental data and limitations of the model space used by Horie and Ogawa.<sup>9</sup> The tentative  $J^\pi$  assignments to states in  $^{53}\text{V}$  in the study by Pronko *et al.*<sup>5</sup> are based upon the lifetime measurements of several of the states and upon considerations of the shell-model predictions and the observed level structures in other  $(f_{7/2})^{n3}$  nuclei.

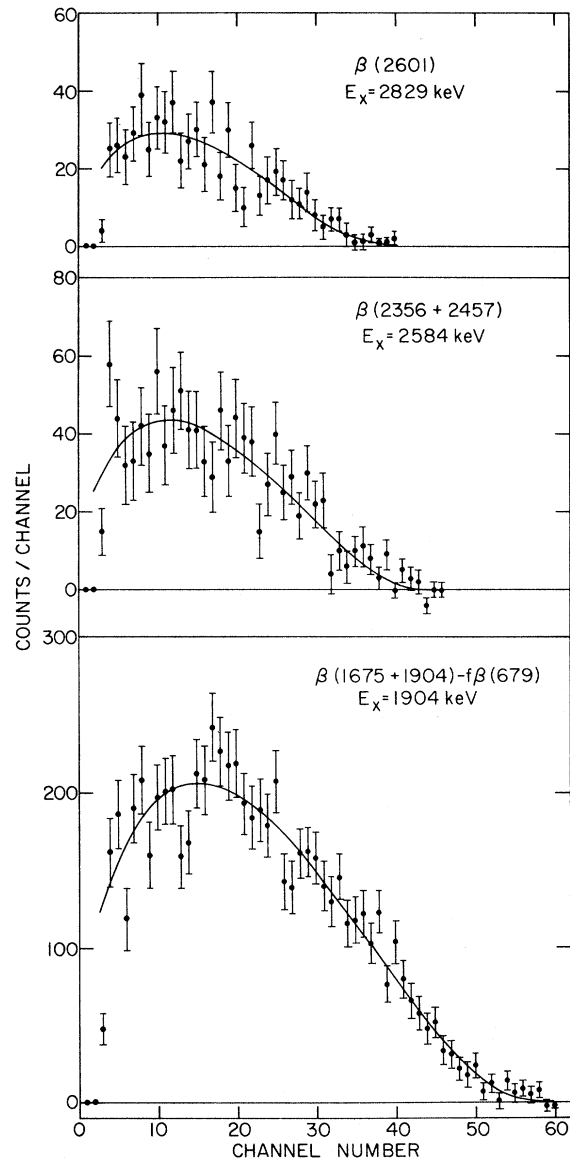


FIG. 6.  $\beta$  spectra feeding the 2829-, 2584-, and 1904-keV  $^{53}\text{V}$  states. The standard shape was fitted to each spectrum (see Table IV).



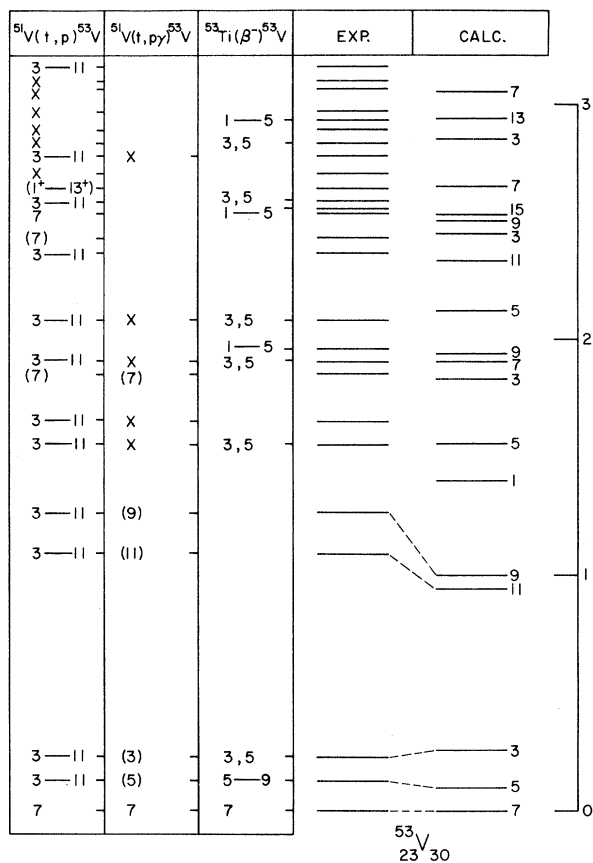


FIG. 7. Summary of the results of this experiment and the  $(t, p)$  studies (Refs. 4 and 5). Comparison is made with the shell-model calculation (Ref. 9). The spin restrictions determined from each study are given in units of half integral spin. All parities are negative unless otherwise specified. An X means that the state was observed but a  $J^\pi$  restriction could not be made. See text.

Horie and Ogawa<sup>9</sup> predicted that the first six states of  $^{53}\text{V}$  are predominantly composed of recoupled  $(f_{7/2})^3$  proton configurations. However, they state that the predicted ground-state structure contains only 70% of this configuration. Although they did not detail the wave function predictions for the other states, it is presumed that there may be configuration mixing in the predicted excited states in addition to the ground state. All of the experimental studies are consistent with the permitted  $J^\pi$  assignments of recoupled  $\pi(f_{7/2})^3$  configurations for the first five observed states of  $^{53}\text{V}$ .

Since it is assumed that the ground state of  $^{53}\text{Ti}$  is predominantly a  $\pi(f_{7/2})^2\nu(p_{3/2})^{-1}$  configuration, the Gamow-Teller  $\beta$  decay will proceed mostly to  $p_{1/2}$  or  $p_{3/2}$  proton configurations in  $^{53}\text{V}$ ; transitions to pure recoupled  $\pi(f_{7/2})^3$  states are forbid-

TABLE V. Mass excess of  $^{53}\text{Ti}$  (in MeV) and comparison with various predictions.

Experiment <sup>a</sup>	$-46.84 \pm 0.10$
Dauids <sup>b</sup> (shell model)	-46.50
Myers <sup>c</sup> (droplet model)	-45.29
Groote, Hilf, and Takahashi <sup>c</sup> (droplet model)	-46.62
Seeger and Howard <sup>c</sup> (liquid drop model)	-46.4
Liran and Zeldes <sup>c</sup> (shell model)	-46.33
Beiner, Lombard, and Mas <sup>c</sup> (energy-density method)	-46.1
Janěcke <sup>c</sup> (Garvey-Kelson relation)	-46.53
Comay and Kelson <sup>c</sup> (Garvey-Kelson relation)	-46.50
1974 mass adjustment <sup>d</sup>	-46.26

<sup>a</sup> Present work.

<sup>b</sup> C. N. Davids, Phys. Rev. C **13**, 887 (1976).

<sup>c</sup> S. Maripuu, At. Data Nucl. Data Tables **17**, 487 (1976), 1975 Mass Excess Predictions.

<sup>d</sup> A. H. Wapstra, K. Bos, and N. B. Gove, 1974 Supplement to the 1971 Atomic Mass Adjustment (private communication, F. J. D. Serduke).

den. By virtue of their relatively low  $\log ft$  values, the 1904-, 2584-, and 2829-keV states are good candidates for having large  $p_{3/2}$  or  $p_{1/2}$  proton configurations.

There is strong evidence that the 127-keV state can almost totally be attributed to a recoupled  $\pi(f_{7/2})^3$  configuration since there appears to be no  $\beta$  feeding to this state. Single-particle  $M1$  transitions are absolutely forbidden between recoupled  $\pi(f_{7/2})^3$  states. If the ground state of  $^{53}\text{V}$  were also a pure recoupled  $\pi(f_{7/2})^3$  state, the  $\gamma$ -ray transition mode between these states would be  $E2$ . If this were the case, deexcitation of the 127-keV state via internal conversion would result in an inferred  $\beta$  feeding to this state on the order of 6 times per 100 disintegrations. This corresponds to a  $\log ft$  value of 6.6, not significantly different from the assigned lower limit. However, as mentioned previously, the measurement of the lifetime of the state by Pronko *et al.*<sup>5</sup> indicates that the state deexcites predominately by an  $M1$  transition. It should be pointed out that the  $M1$  strength is  $\geq 0.02$  single-particle units.

The  $\log ft$  value of the decay to the 228-keV state indicates that this state may have a large contribution from a recoupled  $\pi(f_{7/2})^3$  configuration. The lifetime measurements of states in  $^{53}\text{V}$  by Pronko *et al.*<sup>5</sup> indicated that an  $M1$   $\gamma$ -ray transition from the 228-keV state to the 127-keV state has a strength of at least  $2.3 \times 10^{-3}$  single-particle units. If there is significant  $E2$  mixing for this transition, internal conversion for this particular branch may be of some significance.

Table V compares the measured mass excess of  $^{53}\text{Ti}$  with various predictions.

In summary, the study of the  $\beta$  decay of  $^{53}\text{Ti}$  provides further information on the structure of  $^{53}\text{V}$ . It has restricted possible  $J^\pi$  assignments to states observed in the decay. Further information on multipole mixing ratios and unambiguous  $J^\pi$  assignments for the  $^{53}\text{V}$  states, particularly the

127- and 228-keV states, are needed. This would provide further insight into the structure of states in  $^{53}\text{V}$  and the  $^{53}\text{Ti}$  ground state.

The authors wish to acknowledge valuable discussions with D. Kurath, and wish to thank S. Tabor for helpful comments.

<sup>†</sup>Work performed under the auspices of the Energy Research and Development Administration.

\*Thesis student at Argonne National Laboratory from the University of Texas at Austin. Present address: Department of Physics, The Florida State University, Tallahassee, Florida 32306.

<sup>‡</sup>Alfred P. Sloan Foundation Fellow.

<sup>§</sup>Thesis student at Argonne National Laboratory from the University of Texas at Austin. Present address: Cyclotron Laboratory and Physics Department, Michigan State University, East Lansing, Michigan 48824.

<sup>1</sup>C. N. Davids, S. L. Tabor, E. B. Norman, R. C. Pardo, and L. A. Parks, *Phys. Rev. C* **14**, 1601 (1976).

<sup>2</sup>W. M. Howard, W. D. Arnett, D. D. Clayton, and S. E. Woosley, *Astrophys. J.* **175**, 201 (1972).

<sup>3</sup>A. G. W. Cameron, in *Annual Review of Astronomy and Astrophysics*, edited by Leo Goldberg (Annual Reviews, Palo Alto, 1970), Vol. 8, p. 179.

<sup>4</sup>S. Hinds, H. Marchant, and R. Middleton, *Phys. Lett.* **24B**, 34 (1967).

<sup>5</sup>J. G. Pronko, T. T. Bardin, and J. A. Becker, *Phys. Rev. C* **13**, 608 (1976).

<sup>6</sup>J. Vervier, *Phys. Lett.* **24B**, 603 (1967).

<sup>7</sup>J. Vervier, *Nucl. Phys.* **78**, 497 (1966).

<sup>8</sup>J. B. McGrory, *Phys. Rev.* **160**, 915 (1967).

<sup>9</sup>H. Horie and K. Ogawa, *Nucl. Phys.* **A216**, 407 (1973).

<sup>10</sup>L. A. Parks, C. N. Davids, B. G. Nardi, and J. N. Worthington, *Bull. Am. Phys. Soc.* **21**, 633 (1976); L. A. Parks, Ph.D. thesis, University of Texas at Austin, 1976 (unpublished); and (unpublished).

<sup>11</sup>J. Rapaport, *Nucl. Data* **B3**, 85 (1970).

<sup>12</sup>N. B. Gove and M. J. Martin, *Nucl. Data* **A10**, 205 (1971).

<sup>13</sup>K. Okano, Y. Kawase, and S. Uehara, *J. Phys. Soc. Jpn.* **30**, 1231 (1971).